Gain analysis of vertical-cavity surface-emitting laser for long optical fiber communication

FATEN ADEL ISMAEL CHAQMAQCHEE*
Department of Physics, Faculty of Science and Health, Koya University, University Park, Danielle Mitterrand Boulevard, Koya KOY45, Kurdistan Region, F.R. Iraq

Dilute nitride semiconductors are indispensable for today's optoelectronic devices such as semiconductor lasers and optical amplifiers in the 1300 nm wavelength band used for fiber optic communication systems. These have led to the invention of GaInNAs/GaAs for such applications. Vertical cavity surface emitting lasers (VCSELs) are attractive devices as potential lower manufacturing cost and high performance emitters for optical fiber communication systems. These devices consist of quantum wells QWs that enclosed between standard top and bottom epitaxially grown distributed Bragg reflectors (DBRs). Experimental results for GaInNAs/GaAs VCSEL as output power light-current-voltage (LIV) in continue wave CW and pulsed measurements are presented. Extracted room temperature peak amplitude for VCSEL, laser and VCSEL plus laser at fixed bias current of 10 mA and various input signal power are performed. In addition, GaInNAs/GaAs VCSELs exhibit a single longitudinal lasing mode due to the short cavity cross section area, which tends to limit the output power of the fundamental mode gain around 10 dB is obtained.

(Received January 2, 2020; accepted August 18, 2020)

Keywords: VCSELs, GaInNAs/GaAs, Quantum well, Optical gain, LIV characterization

1. Introduction

Dilute III-N-V semiconductor alloys are becoming increasingly important for optoelectronic devices applications, such as lasers, modulators, photodetectors and optical amplifiers for the 1.3 μm window of the optical fiber communication systems. One potentially important material for such applications are the quaternary alloy GaInNAs [1-3] and the quinary alloy GaInNAsSb [4-6]. GaInNAs may be grown pseudomorphically on GaAs, allowing the use of high quality Al(Ga)As/GaAs distributed Bragg reflectors (DBRs), with potential cost advantages over InP-based approaches due to their electronic structure can maintain stronger carrier confinement even at high temperatures [7]. Dilute nitride structures have already found applications in several devices, such as high performance laser diodes among which are cavity surface emitting lasers (VCSELs) emitting in the 1.3 μm window. A VCSEL with a high number of top DBR layers enables it to operate in the linear regime above threshold currents [8]. VCSELs are important components in optical fiber networks. Optically pumped structures at 1.3 μm wavelength operation have also been realized [9,10]. VCSELs are becoming the component of choice for numerous applications over conventional edge emitting lasers (EELs) including data communication, optical interconnections and memory and sensors [11]. It also allows for on chip testing techniques, single wavelength amplification, and two dimensional array fabrication; hence lowering the power consumption and manufacturing cost.

VCSELs are driven above lasing threshold and studied at the short wavelengths of 850 and 980 nm [12,13] and at long wavelengths of 1300 and 1550 nm [14,15] windows. They show some very interesting characteristics derived from the Fabry Perot cavity. The cavity consists of nine quantum wells (QWs) distributed equally in three stacks forming a cavity $3\lambda/2n_c$ long, where n_c is the refractive index of cavity. Holes and electrons are injected through the un-doped top and bottom mirrors, respectively, pass through the QWs, recombine and generate photons.

In this study, we have demonstrated the operation of VCSELs devices based on GaInNAs/GaAs for metro and access networks applications. The results of the calculated reflectivity spectrum, the photoluminescence (PL) peak, the output power light-current-voltage (LIV), the voltage-electroluminescence (V-EL) characteristics and the amplitude as a function of the laser power are presented at room temperature. An optical gain at around 10 dB is obtained on GaInNAs/GaAs VCSEL under using optical and electrical injection at applied power of 1 mW.

2. Material and method

The fabrication procedure for VCSELs required a number of lithography steps, including dry and wet etching steps to facilitate wafer bonding structure. The proposed pad size of GaInNAs/GaAs VCSELs is 120 μm×200 μm, where pad to pad metal separation is around 50 μm. The device has a fixed mirror diameter (first mesa etch) of 10 μm, while the radius of the second mesa is 60 μm. Further details on VCSEL structure can be found elsewhere [16]. The total number of photolithography steps for all the devices could be reduced by combining

the SiO_2 or SiNx hard mask etch steps, including the contact window definition. Finally, multilayer metallization system of titanium-platinum-gold (Ti/Pt/Au) was used. Titanium is used to promote adhesion between substrates and sputtered gold films, which can diffuse up to the gold surface after annealing and then degrade the wire bondability [17].

The GaInNAs/GaAs VCSEL structure coded G0418 includes three elements of top DBRs, quantum wells QWs and bottom DBRs as shown in Fig. 1(a). The bottom DBR mirrors constitutes 24-pairs $Al_{0.98}Ga_{0.02}As$/GaAs resulting in over 99.9% reflectivity. The top DBR mirrors consists of 21-pairs of undoped $Al_{0.8}Ga_{0.2}As$/GaAs quarter wavelength thick layers to provide greater than 99% reflectivity for the optical microcavity as well as for gain region. The choice of 0.8 and 0.98 Al content in the DBRs was to allow 0.98 Al for the oxidation layer. The gain region is made of nine QWs that are distributed equally in three stacks of 7 nm thick $Ga_{0.65}In_{0.35}N_{0.02}As_{0.98}$ QWs separated by 20 nm thick GaAs. The QWs were positioned at the antinodes of the field to provide resonant periodic gain and to maximize available gain. Fig. 1(b) shows room temperature photoluminescence (PL) peak intensity measurement with calculated mirror reflectivity by the transmission matrix method [18]. The spectral position of the PL peak emission coincides with the dip in the stopband of the DBR at around 1270 nm.

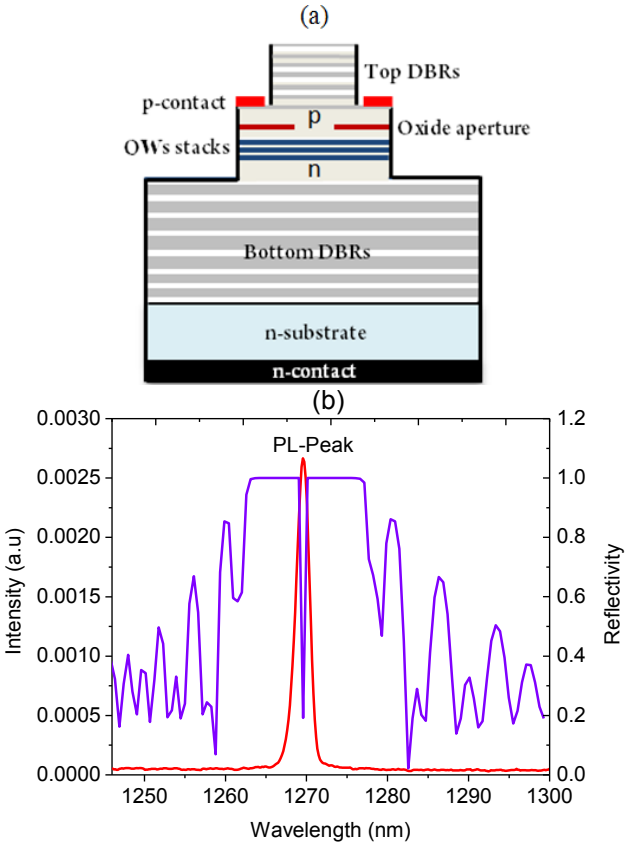

Fig. 1. Room temperature GaInNAs VCSEL samples with their (a) top DBRs, QWs and bottom DBRs structure and (b) photoluminescence PL spectra (red) with theoretically calculated reflectance spectrum (blue) (color online)

Electrical injection, continue wave CW and pulsed measurements were performed on the GaInNAs/GaAs VCSEL devices, making measurements with a power meter, fast detector, and photomultiplier tube according to the pulse width and repetition rate. The devices have been fabricated with different diameters. The small size of VCSELs (their small cross-sectional area) makes the threshold current density easy to achieve with amplification was observed on devices.

3. Experimental details

The characterization of gain was measured under continuous-wave (CW) pumping using the fiber-based system sketched in Fig. 2. A 980 nm fibre pigtailed single mode diode laser (1999 PLM 980 nm pump module) is used for VCSEL excitation through a 980 nm isolator and an optical coupler. The output power from the laser is about 810 mW and is reduced to less than 250 mW at the sample due to the losses through fibres. The laser signal passes through an isolator to prevent reflections and instabilities. The long focus fibre (with radius of 8 μm) is brought very close to the surface of the sample. The device under test is perfectly mounted on the temperature controlled heatsink fixed in a simple two-axis gimbal mount. The circulator is used as a special fibre optic component to separate the amplified signal from the input signal and pump light. The circulator usually has three ports. The first port is connected to the optical attenuator and, the second one is connected to the coupler and the last one is connected to the optical spectrum analyser, which measures the optical power as a function of wavelength or frequency. Therefore, the light intensity is exhibited as a function of wavelength over a fixed wavelength range. The amplified signal can be also detected using an optical power meter. The tunable laser, along with the optical spectrum analyser (OSA) are employed to investigate the VCSEL spectrum and peak optical gain under low output power.

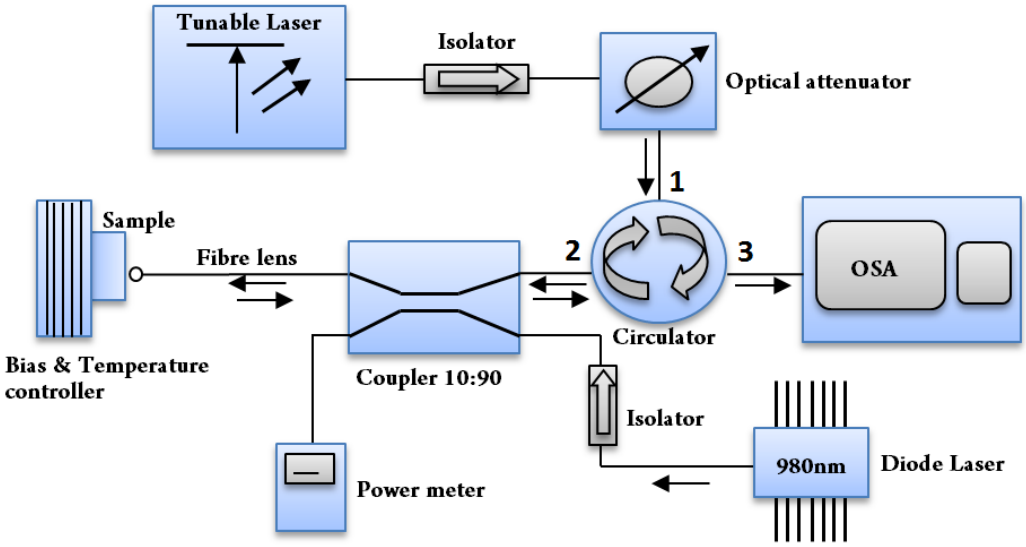

Fig. 2. Schematic of the VCSEL experimental setup used for top emitting characterization system (color online)

4. Result and discussion

The output power light-current-voltage (LIV) and voltage-electroluminescence (V-EL) characteristics of the VCSEL have been measured at room temperatures. Figure 3(a) shows the temperatures of T=14 and 20 ºC output characteristics of emitting VCSEL at a wavelength of 1.3 µm for an aperture diameter of 10 µm and the second mesa etch diameter is 60 µm. The emission occurred for an applied voltage and direct bias current DC as low as 2.8 V and 0.8 mA, respectively. The maximum single mode output power was 0.06 nW at 10.8 mA for the 1.286 µm VCSEL. This can be seen by the slightly increased output power when the temperature of the device increased into 14 ºC. As a result, no threshold current was observed and thus the device emitted spontaneously. In addition, we have measured the integrated EL intensity for different pulse widths using photomultiplier tube (PMT) system. By reducing the pulse width from 80 to 600 µs, small of lasing were noticed from the VCSEL as shown in Fig. 3(b).

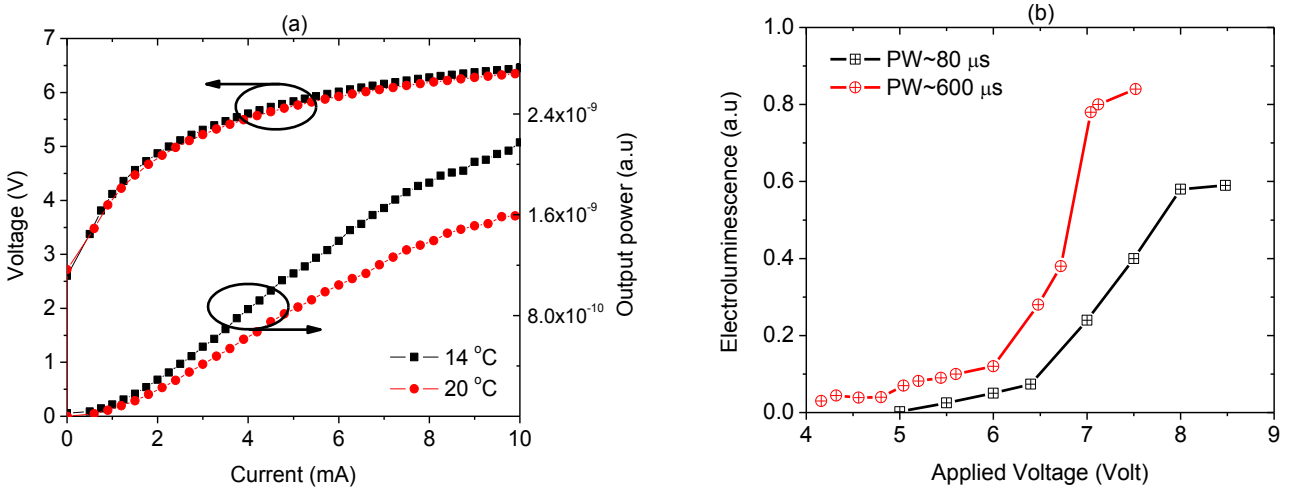

Fig. 3. Comparison of light intensity of VCSEL sample with (a) L-I-V under DC operation with aperture diameter of 10 µm and at T=14 and 20 ºC (b) EL-V under pulsed operation of 80 and 600 µs T=15 ºC (color online)

The spectra of the VCSEL, input signal and the combined VCSEL plus input signal as a function of input signal power are shown in Fig. 4. The chip temperature was held constant at T=14 ºC. The emission spectra of a 60 µm device were measured in CW operation. The bias current was fixed at I_{bias}=14 mA. The tuned laser wavelengths were scanned from 1260 to 1315 nm using an input signal power from P=1 to 6 mW. As the power of the input signal is increased, the carrier consumption increases. As depicted in Fig. 5, gain about 9.7 dB under power of P=1 mW was observed from the device with an increasing input signal power up to a maximum of P=6

mW. Further improvements in gain characteristic and device performance will be expected by optimizing the VCSEL structure at 1300 nm and reducing the device length for lower operating voltage and bias current. Additionally, VCSEL might be required a nano or few milliwatts of injected optical power to obtain high gain [19].

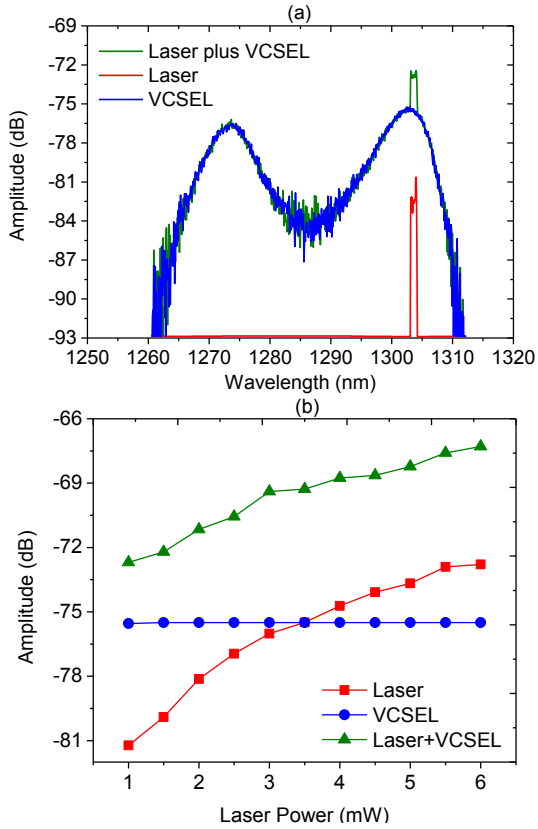

Fig. 4. The spectra of VCSEL, tunable laser signal and the combined of VCSEL plus tunable laser signal measurements at fixed bias current of I_{bias}=14 mA and T=14 °C with (a) applied power of P=1 mW and (b) various input signal powers and for fixed peak spectrum of λ=1303.61 nm (color online)

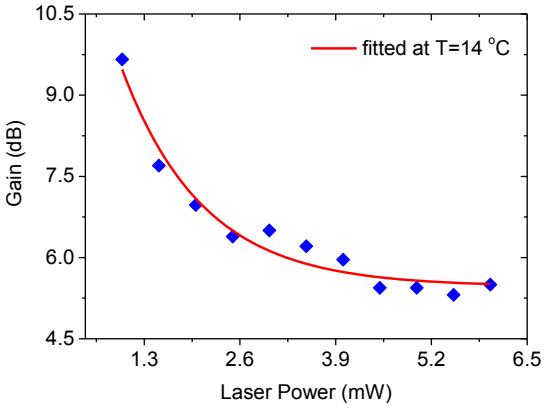

Fig. 5. Gain versus laser power that extracted from peak emission spectra of VCSEL, tunable laser signal and the combined of VCSEL plus tunable laser signal at fixed bias current of I_{bias}=14 mA, power of P=1 mW and T=14 °C. Polynomial fitted gain measurements (color online)

5. Conclusion

VCSELs have advantages compared to edge-emitting lasers due to their lower cost and lower consumption power. In this paper, we have demonstrated low intensity gain at around 10 dB based on GaInNAs/GaAs VCSEL. For future devices, a standard oxidation of the high Al-content layers should be considered for a better carrier and light confinement. With electrical injection, the structure with a large number of quantum wells (QWs) often suffers from the issue of carrier transport. The current injection into the active region is not uniform which may lower the lasing threshold. Future improvements can be achieved by adapting the well-established 1300 nm VCSEL technology.

Acknowledgements

This work was funded by higher ministry and scientific research in Baghdad-Iraq. FC highly appreciates the support of University of Essex in Colchester-UK through this research. FC also acknowledges department of Physics at Koya University in Kurdistan region-Iraq for enabling this study.

References

[1] M. Kondow, K. Uomi, A. Niwa, T. Kitatani, S. Watahiki, Y. Yazawa, Jpn. J. Appl. Phys. **35**, 1273 (1996).
[2] I. A. Buyanova, W.M. Chen, B. Monemar, MRS Internet Journal of Nitride Semiconductor Research **6**, 2 (2001).
[3] F.A. I. Chaqmaqchee, S. Mazzucato, M. Oduncuoglu, N. Balkan, Y. Sun, M. Gunes, M. Hugues, M. Hopkinson, Nanoscale Research Letters **6**, 1 (2011).
[4] A. Aho, V. M. Korpijärvi, R. Isoaho, P. Malinen, A. Tukiainen, M. Honkanen, M. Guina, Journal of Crystal Growth **438**, 49 (2016).
[5] F. A. I. Chaqmaqchee, S. A. A. Salh, M. F. M. Sabri, ZANKO Journal of Pure and Applied Sciences **32**, 87 (2020).
[6] M. Gebski, D. Dontsova, N. Haghighi, K. Nunna, R.Yanka, A. Johnson, R. Pelzel, J. A. Lott, OSA Continuum **3**, 1952 (2020).
[7] H. Li, P. Wolf, X. Jia, J.A. Lott, D. Bimberg, Applied Physics Letter **111**, 243508 (2017).
[8] F. A. I. Chaqmaqchee, ZANCO Journal of Pure and Applied Sciences **31**, 14 (2019).
[9] K. D. Choquette, J. F. Klem, A. J. Fischer, O. Blum, A. A. Allerman, I. J. Fritz, S. R. Kurtz, W. G. Breiland, R. Sieg, K. M. Geib, J. W. Scott, R. L. Naone, Electronic Letters **36**, 1388 (2000).
[10] F.A. Chaqmaqchee, Arab J. Sci. Eng. **39**, 5785 (2014).
[11] G. Knowles, R. Fehse, S. Tomic, S. J. Sweeney, T. E. Sale, A. R. Adams, E. P. O'Reilly,

G. Steinle, H. Riechert, IEEE Journal of Selected Topics in Quantum Electronics **9**, 1202 (2003).
[12] K. Szczerba, P. Westbergh, M. Karlsson, P. A. Andrekson, A. Larsson, Electronics Letters **49**, 953 (2013).
[13] A. Liu, P. Wolf, J. A. Lott, D. Bimberg, Photonics Research **7**, 121 (2019).
[14] N. Laurand, S. Calvez, M. D. Dawson, A. C. Bryce, T. Jouhti, J. Kontinnen, M. Pessa, IEEE J. of Quant. Elect. **41**, 642 (2005).
[15] R. Lewen, K. Streubel, A. Karlsson, S. Rapp, IEEE Photo. Tech. Letts. **10**, 1067 (1998).
[16] F. A. I. Chaqmaqchee, Aro- The Scientific Journal of Koya University **8**, 107 (2020).
[17] G. G. Harman, Wire bonding in microelectronics materials, processes, reliability and yield, 2nd edition, McGraw-Hill, New York, 1997.
[18] H. A. Macleod, Thin-film optical filters, Adam Hilger Ltd., 1986.
[19] S. B. Lisesivdin, N. A. Khan, S. Mazzucato, N. Balkan, M. J. Adams, V. M. Korpijärvi, M. Guina, G. Mezosi, M. Sorel, Nanoscale Research Letters **9**, 1 (2014).

* Corresponding author: faten.chaqmaqchee@koyauniversity.org